Conf-920247--1

FLUXLESS LASER SOLDERING FOR ELECTRONIC PACKAGING*

by

F. Michael Hosking and David M. Keicher
Center for Solder Science and Technology
Sandia National Laboratories
Albuquerque, New Mexico 87185

SAND--91-2606C

DE92 003958

ABSTRACT

Conventional soldering typically requires the use of reactive fluxes to promote wetting. The resulting flux residues are removed primarily with halogenated or chlorofluorocarbon (CFC) solvents. With the mandated phaseout of CFCs by the year 2000, there has been a concentrated effort to develop alternative, environmentally compatible manufacturing and cleaning technologies that will satisfy the restrictions placed on CFCs, but still yield high quality product. Sandia National Laboratories is currently evaluating a variety of alternative fluxless soldering technologies which can be applied to electronic packaging. Laser soldering in a controlled atmosphere has shown great potential as an environmentally compatible process. The effects of laser heating with a 100 watt CW Nd:YAG laser, joint design, and base/filler metal reactions on achieving fluxless wetting with good metallurgical bonds were examined. Satisfactory Ni-Au plated Kovar® solder joints were made with 80In-15Pb-5Ag and 63Sn-37Pb (wt. %) solder alloys in a slightly reducing cover gas. Wetting generally increased with increasing laser power, decreasing laser beam spot size, and decreasing part travel speed. The materials and processing interaction effects are identified and discussed.

KEYWORDS:
Environmentally Compatible Electronic Manufacturing
Fluxless Laser Soldering
Controlled Atmosphere

INTRODUCTION

There are increasing concerns over the environmental effects of chlorofluorocarbons (CFCs) throughout the international scientific and engineering community. CFCs have been identified as a source of stratospheric ozone depletion and are seriously affecting both the environment and human health [1-3]. The most celebrated example of ozone depletion is the ozone hole which has developed over the Antarctic and is a result of the emissions from fully halogenated CFCs and halons. An international agreement, the Montreal Protocol, was formalized to address this particular problem. The Clean Air Act of 1990 was passed to enforce the principles of the Montreal Protocol within the United States. The phaseout of controlled CFCs must be currently completed by the year 2000. Other fully halogenated CFCs, carbon tetrachloride, and methyl chloroform are also affected by the Protocol and Clean Air Act controls [4]. These international restrictions on CFCs will significantly impact the electronics industry and require the development of more environmentally compatible cleaning and manufacturing techniques.

Cleaning is a major element in electronic soldering. An electronic package is typically populated with many devices (surface mount devices, capacitors, resistors, chip carriers, leaded devices, etc.) that are soldered to a printed circuit board. Conventional soldering typically requires a flux to promote wetting of the base metal by the solder alloy [5]. The flux has three functions. The first is to chemically remove surface oxides and provide a protective layer over the cleaned surfaces during soldering. The second is to

---

* The work is being conducted by Sandia National Laboratories and is supported by the U.S. Department of Energy under contract number DE-AC04-76DP00789.

DISCLAIMER

DISCLAIMER

assist heat transfer and remove reaction products. The third is to affect interfacial surface tensions such that spreading of the molten solder is enhanced. Flux residues must be subsequently removed from the soldered assembly. Although the residues are generally nonconductive, they are corrosive and could create a long term reliability problem, especially for applications where extended storage or operation in uncontrolled environments occurs. These conditions make residue removal mandatory. Rosin-based flux residues are typically removed with halogenated or CFC solvents. This practice is changing because of the restrictions imposed by the Montreal Protocol and the Clean Air Act. New solvents, fluxes, and cleaning methods are consequently being developed to satisfy the CFC phaseout. Terpene solvents, aqueous based cleaning, water soluble fluxes, and low solids ("no clean") fluxes have shown promise. Alternative, fluxless soldering technologies are also being developed to complement the above activities. Fluxless soldering will not eliminate the need for cleaning during electronic manufacturing, but it will help to reduce the total number of cleaning steps and the volume of solvent waste consequently generated.

The Center for Solder Science and Technology at Sandia National Laboratories (SNL) has a very active program underway to characterize and demonstrate fluxless soldering alternatives [6-7]. The DOE Office of Technology Development is funding the SNL effort and is especially interested in developing faster, better, cheaper, and safer processes and materials that can satisfy the increasing need for environmental restoration and waste minimization. The work has focused primarily on controlled atmosphere soldering (vacuum, inert/reducing gases, reactive plasmas, and activated acid vapors), thermomechanical surface activation soldering (laser, ultrasonic, and solid state), and protective coatings (metallizations and organic inhibitors). These diverse technologies are being jointly developed to yield a variety of processes from which to choose, since there is no generic or "drop-in" fluxless soldering operation that can be universally applied during electronic manufacturing. The selected process must be compatible with not only the base and filler metals, but also with any neighboring materials. Sensitivity to lasers, infrared heating, or reactive plasmas is of special concern since they could degrade the functional performance of a component. Materials such as alumina, glass frits, epoxy, polyester, phenolic, polyimide, plastics, and conformal coatings can be damaged by exposure to these more active processes.

Laser soldering typically involves the melting of a preplaced or fed solder preform with a directed CO_2 or Nd:YAG laser beam [8-9]. Rapid heating and cooling of the solder joint produces a very fine microstructure with reduced intermetallic formation. The process is highly automated and offers improved process control. Higher strength solder joints are possible since the localized heating of a laser allows the use of higher melting solder alloys without damaging nearby materials. Solder mixing with other solder joints of different alloy compositions can also be avoided because of this localized heating effect. This paper will discuss the SNL development of fluxless laser soldering [10]. The work emphasized the evaluation of hermetic closure joints, although the technology can also be readily applied to leaded and surface mounted devices. Fluxless laser soldering can also enhance product reliability by eliminating entrapped, corrosive flux residues within a sealed package. The effects of Nd:YAG laser heating on producing fluxless solder joints between metallized substrates in a controlled atmosphere were investigated.

EXPERIMENTAL PROCEDURE

Laser soldering is adaptable to most solder joint geometries. When developing the working limits of the process, it is necessary to first characterize the energy distribution of the laser beam. The effect of the base surface on the absorption of the laser energy is also important and determines where the laser beam is focused. For example, Au surfaces are highly reflective at the fundamental wavelength of a Nd:YAG laser and are difficult to heat quickly to the desired soldering temperature. This condition consequently presents a problem when soldering Au-plated components. Since solder alloys typically have better absorption properties than Au, the solution is to direct the laser beam on the solder alloy and conduct heat from the solder to the base surface.

The work reported in this paper investigated the fabrication of laser soldered closure joints without fluxing. A 100 watt, continuous wave (CW) Nd:YAG laser was used to make prototypic joints for visual and metallographic analyses. The Nd:YAG laser emits light at a wavelength of 1.06 µm and is ideal for soldering because of the relatively high absorption of the laser energy by solder alloys. The laser system was equipped with a computer controlled x-y directional stage and a heating platform for preheating of the test samples. The system also had a coaxial video monitor to assist in alignment of the laser beam relative to the target area and for viewing of the immediate region around the laser heated zone. A schematic of the system is shown in Figure 1.

A parametric test matrix was designed to examine the feasibility of laser soldering Ni-Au plated Kovar closure joints. Kovar (nominally 53Fe-29Ni-17Co-0.5Mn, wt. %) is generally very difficult to directly wet with solder unless a very aggressive, corrosive flux is applied. Since most active fluxes are not permitted during electronic soldering, Kovar is typically electroplated with a 5.0 µm (200 µin.) layer of Ni followed by a 1.2 µm (50 µin.) overplating of Au to enhance its solderability. This metallization scheme is also critical to the success of fluxless soldering and was used throughout the study. The noble Au surface prevents oxidation of the underlying metal before and during soldering.

Two solder alloys were evaluated; 80In-15Pb-5Ag and 63Sn-37Pb, wt. %. The 80In-15Pb-5Ag alloy has a melt range of 142 to 149°C, while the 63Sn-37Pb alloy is a eutectic and melts at 183°C. Solder preforms nominally 0.76 mm (0.030 in.) wide and 0.125 mm (0.005 in.) thick were prepared from commercially supplied stock. Two flat Ni-Au Kovar plates of different thicknesses were fixtured perpendicular to each other (L-joint) with a 45° taper on the thicker of the two mating surfaces to accommodate the placement of the solder preform. The base plate thicknesses were 0.76 mm (0.030 in.) and 1.78 mm (0.070 in.). The fixtured samples (with preforms) were preheated to 110°C prior to soldering. Soldering was done without fluxing in a protective reducing gas cover of 3 to 5 vol. % hydrogen in argon.

Laser power, laser beam focused spot diameter, and part travel speed were the experimental variables. The test matrix was a two level factorial design with a limited response surface to estimate linear and interaction effects. Each test condition was replicated twice, except for the midpoint which was repeated four times. A separate set of experiments was randomly conducted with each solder alloy. The laser power was varied from 30 to 100 watts, the laser spot diameter was varied from 0.38 to 0.88 mm (0.015 to 0.035 in.), and the part travel speed was varied from 2 to 17 mm-sec^{-1} (5 to 40 in-min^{-1}). The experimental midpoint was 65 watts, 0.63 mm (0.025 in.) laser spot size, and a 9.5 mm-sec^{-1} (22.5 in-min^{-1}) travel speed. The specific test conditions are listed in Table 1. The soldered samples were visually inspected for solder wetting and flow. The joints which exhibited satisfactory wetting were then selected for sectioning and microstructural analysis.

RESULTS AND DISCUSSION

The energy distribution of the laser beam was characterized before proceeding with the fluxless soldering evaluation. The laser beam cross-sectional energy distribution was determined for the various focused laser beam spot diameter sizes specified in the test matrix. The energy distribution was measured using a scanning aperture technique (Figure 2). A 25 µm diameter Au-plated diamond aperture was scanned at a constant speed through the center of the laser beam to characterize its distribution. A typical energy distribution curve is shown in Figure 3 for a 0.38 mm diameter spot size. Similar curves can be produced with the other spot sizes. The laser beam spot size was determined by transmitting an electrical signal proportional to the laser energy through the aperture and recording it on a digital oscilloscope for analysis. Focused spot diameters were measured for focus positions over approximately a 25 mm range in the vertical direction. The focused spot size was then plotted as a function of the distance from the workpiece to the objective lens for several power levels (Figure 4). The position of the objective lens from the sample for a given focused laser beam spot size was then extracted from these plots.

Previous experiments [8] revealed that the reflective properties of Au plating would inhibit the absorption of the laser energy into the base Kovar parts. Au has a relative absorption factor of 0.012 while the 63Sn-37Pb and 80In-15Pb-5Ag alloys have an absorption factor of 0.28, a nominal absorption increase of over twenty. The closure joint was consequently designed to utilize the absorption properties of the solder to conduct the laser energy to the solder joint region. Solder preforms with a 0.76 x 0.125 mm cross-section were placed into the tapered joint just prior to soldering with the 0.125 mm side facing the laser beam.

To promote solder wetting without fluxing, a slightly reducing, controlled atmosphere was introduced over the fixtured parts to protect the base and solder alloy surfaces during heating. The cover gas prevents the probable oxidation in air of the underlying Ni layer and dewetting by the molten solder alloy. Thermodynamic data suggests that the higher temperatures of laser soldering in an inert or reducing atmosphere can significantly enhance the reduction of most metallic oxides (eg. Cu, Ni, Fe, Sn, and Pb) [11-12]. This effect is especially noticeable above 350°C. Since the laser heated region is very localized, the process is ideal for fluxless soldering.

The Ni-Au plated Kovar solder joints were visually inspected to assess the quality of solder wetting/spreading. The wetting results for the 80In-15Pb-5Ag and 63Sn-37Pb alloys are summarized in Figure 5. Wetting was qualitatively ranked from poor to good and was dependent on the degree of solder joint filled. Generally better wetting was observed with 63Sn-37Pb than 80In-15Pb-5Ag. The results were consistent with the wetting behavior normally expected during conventional soldering of these alloys on Au with a flux.

Good solder joints were obtained at the higher laser power setting for both solder alloys. Poor wetting generally occurred at the lower 30 watt power level with very irregular to negligible solder flow. The higher power input generally contributed to greater heating and could potentially degrade heat sensitive components if they were located next to the joint. The objective, therefore, was to adjust the heating parameters such that an acceptable joint is produced without damaging the performance of the device.

Wetting was not as good on the midpoint samples. Only partial filling of the joints was observed. After conducting these midpoint experiments, however, the laser beam spot size was discovered to be 0.25 mm larger than the experimentally designed value of 0.63 mm. The size difference could affect the wetting results since the larger spot size would diffuse the heat affected zone and produce less heating. The smaller spot size with constant laser power and part travel speed should produce slightly better heating and consequently better wetting. Wetting could be further improved by reducing the travel speed

There were two exceptions to the general trends noted above. The first was that the 30 watt, 0.38 mm, 2.0 mm-sec^{-1}, 63Sn-37Pb samples gave adequate wetting. The smaller laser focused spot size and slower travel speed concentrated the laser energy at the lower laser power setting and effectively heated the 63Sn-37Pb preforms. The same result was not achieved with the 80In-15Pb-5Ag alloy. This wetting difference can be explained by the compositional differences between the two alloys. The second observation was that both solder alloys gave spotty to partial wetting with the 100 watt, 0.88 mm, and 17 mm-sec^{-1} test parameter. The larger spot size and faster travel speed produced less heating and consequently poorer wetting, even at the higher laser power value.

After visually inspecting each laser soldered joint, samples were chosen from those exhibiting adequate or good wetting for metallographic analysis. The samples were electrolytically overplated with approximately 0.1 mm (0.001 in.) of Ni to retain the soft solder edges during sectioning and polishing. The 63Sn-37Pb samples were polished through 1 μm diamond paste followed by vibratory polishing with 0.06 μm colloidal silica. The 80In-15Pb-5Ag samples were similarly prepared without vibratory polishing. Figure 6a shows a Ni-Au plated Kovar and 63Sn-37Pb solder joint that was made at 100 watts with a 0.88 mm laser beam spot size and 2.0 mm-sec^{-1} travel speed. The joint exhibited "good" wetting with a very fine textured microstructure and small Au-Sn and Ni-Sn intermetallic precipitates dispersed throughout the joint. Similar results were observed with the 80In-15Pb-5Ag solder alloy, although wetting was not as extensive as with the 63Sn-37Pb alloy. Figure 6b shows a 100 watt, 0.38 mm spot size, 17.0 mm-sec^{-1} travel speed, 80In-15Pb-5Ag sample. A more detailed microstructural analysis is underway to characterize the effects of laser processing on intermetallic precipitation in the filler metal during and after soldering. These precipitates could affect spreading and the mechanical behavior of the soldered joint.

Excessive intermetallic growth can result during laser reflowing of a solder joint since the process typically requires longer dwell times to remelt the joint. If the dwell time (or heat input) is too long, melting of the base metal can occur. The resulting microstructure is significantly altered and can drastically affect the joint properties. A reflow experiment demonstrating this problem was conducted on Ni-Au plated Kovar and 63Sn-37Pb joints by making multiple passes over a previously laser soldered sample. Electron probe microanalysis revealed that a narrow band of the remaining metallized layer and underlying Kovar was melted during the reflow experiment. Wavelength dispersive x-ray spectrometry identified $AuSn_4$ precipitates throughout the joint and a substantial quantity of feathery $(Ni, Fe, Co)_3Sn_2$ precipitates in the solder where the base surface was melted. The $AuSn_4$ precipitates formed during the initial soldering operation and would affect the as-soldered joint properties while the $(Ni, Fe, Co)_3Sn_2$ precipitates would only influence the properties of the reflowed joint.

SUMMARY

Laser heating has been applied to fluxless soldering of Ni-Au plated Kovar. The effects of processing conditions on producing satisfactory 63Sn-37Pb and 80In-15Pb-5Ag solder joints were determined. The higher laser power, smaller laser beam focused spot size, and slower travel speed gave the best wetting results. Although the process was developed for closure joints, it can be readily applied to attaching leaded and surface mounted devices. The advantages of fluxless laser soldering are: 1) higher joining temperatures and potentially stronger joints, 2) elimination of entrapped corrosive flux residues, 3) compliance with environmental restrictions on hazardous solvent use, and 4) automated processing and process control. The disadvantages of laser soldering include: 1) inhibited absorption of the laser energy by highly reflective materials, 2) conventional geometries may not be necessarily compatible with the process, and 3) overheating can produce unsatisfactory microstructures and affect joint properties.

ACKNOWLEDGEMENTS

The authors would like to acknowledge the microanalytical support of Alice Kilgo and Paul Hlava, the technical input of Jim Jellison, the program support of Joan Woodard and Barry Granoff of SNL's Environmental and Manufacturing R&D Programs Directorate, and Clyde Frank of the DOE Office of Technology Development.

REFERENCES

1. Molina, M. J. and F. S. Rowland, "Stratospheric Sink for Chlorofluoromethanes: Chlorine Atom-Catalyzed Destruction of Ozone", Nature, 249, 810-812 (1974).
2. S. Derra, "CFCs, No Easy Solutions", R&D Magazine, 56-66 (May 1990).
3. S. O. Anderson, "Progress by the Electronics Industry on Protection of Stratospheric Ozone", 40th Electronic Components & Technology Conference Proceedings, IEEE, 1, 222-227 (1990).
4. ICOLP Technical Committee (S. Greene, Chairman), "Aqueous and Semi-aqueous Alternatives for CFC-113 and Methyl Chloroform Cleaning of Printed Circuit Board Assemblies", EPA Report 400/1-91/016, June 1991.
5. Wassink, R. J. K., Soldering in Electronics, Electrochemical Publications, Scotland, 2nd Edition, 204-262 (1989).
6. F. M. Hosking, "Reduction of Solvent Use Through Fluxless Soldering", USAF/DOE International Workshop on Solvent Substitution (Proceedings), Phoenix, Arizona (December 4-7, 1990).
7. Hosking, F. M., D. R. Frear, P. T. Vianco, and D. M. Keicher, "SNL Initiatives in Electronic Fluxless Soldering", Proceedings of the 1st International Congress on Environmentally Conscious Manufacturing, Santa Fe, NM (September 1991).
8. Jellison, J. L. and D. M. Keicher, "Microsoldering and Microminiature Welding with Lasers," International Symposium and Exhibition Microjoining 88, The Welding Institute, Cambridge, UK (1988).
9. C. Lea, "Laser Soldering - Production and Microstructural Benefits for SMT," Soldering & Surface Mount Technology, 2, 13-21 (June 1989).
10. Hosking, F. M. and D. M. Keicher,"Fluxless Soldering of Ni-Au Plated Kovar with a Laser", presented at the Spring 1991 Materials Research Society Symposium, Anaheim, CA (April/May 1991).
11. D. R. Milner, "A Survey of the Scientific Principles Related to Wetting and Spreading", British Welding Journal, 90-105 (March, 1958).
12. Bredzs, N. and C. C. Tennenhouse, "Metal-Metal Oxide -Hydrogen Atmosphere Chart For Brazing or Bright Metal Processing", Welding Journal, Welding Research Supplement, 86-90 (May 1970).

TABLE 1.

Laser Processing Conditions for Soldering Ni-Au Plated Kovar

Laser Power, W	Laser Beam Spot Size, mm	Travel Speed, mm-sec^{-1}
30	0.38	2.0
30	0.38	17.0
30	0.88	2.0
30	0.88	17.0
65	0.88*	9.5
100	0.38	2.0
100	0.38	17.0
100	0.88	2.0
100	0.88	17.0

* Midpoint laser focused spot size was originally designed to be 0.63 mm.

FIGURE CAPTIONS

Figure 1. Process schematic for laser soldering.

Figure 2. Technique for determining the laser beam energy distribution and focused spot size.

Figure 3. Laser beam cross-sectional energy distribution for a 0.38 mm spot size.

Figure 4. Laser beam focused spot size as a function of distance from the lens holder and varying laser power.

Figure 5. Relative wetting of 63Sn-37Pb and 80In-15Pb-5Ag solder alloys on Ni-Au plated Kovar with laser heating in a dilute hydrogen-argon reducing gas [ranking order: poor (1) < spotty (2) < partial (3) < adequate (4) < good (5)].

Figure 6. Optical images of Ni-Au plated Kovar solder joints made with a CW Nd:YAG laser at (a) 100 watts, 0.88 mm spot size, and 2.0 mm-sec^{-1} travel speed with 63Sn-37Pb and (b) 100 watts, 0.38 mm spot size, and 17.0 mm-sec^{-1} travel speed with 80In-15Pb-5Ag.

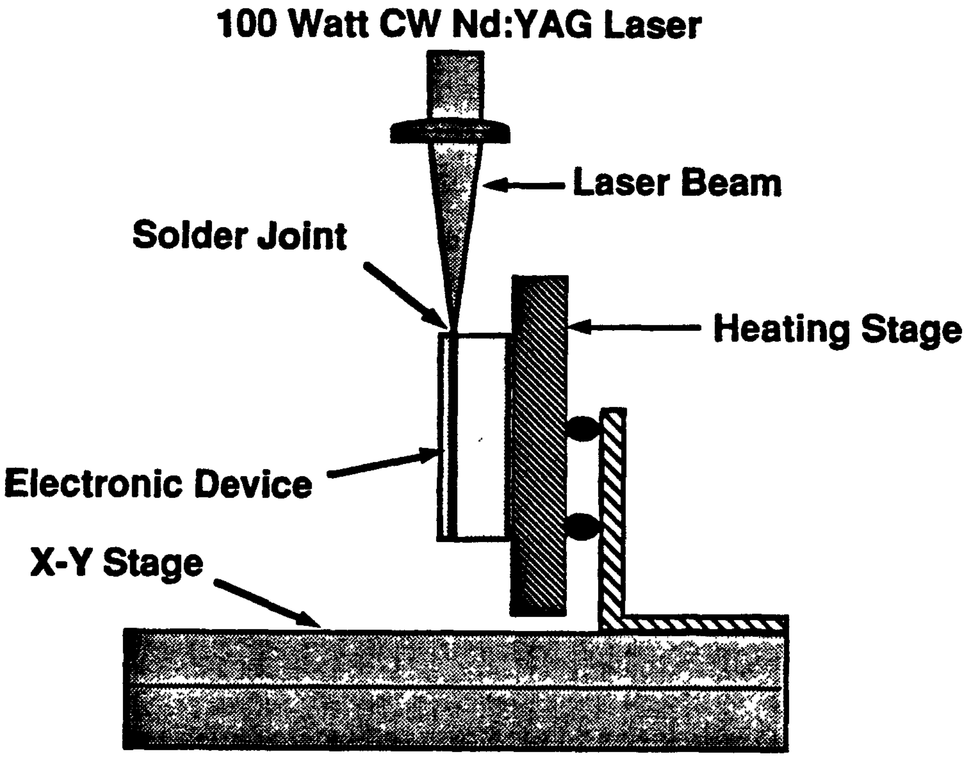

Figure 1.

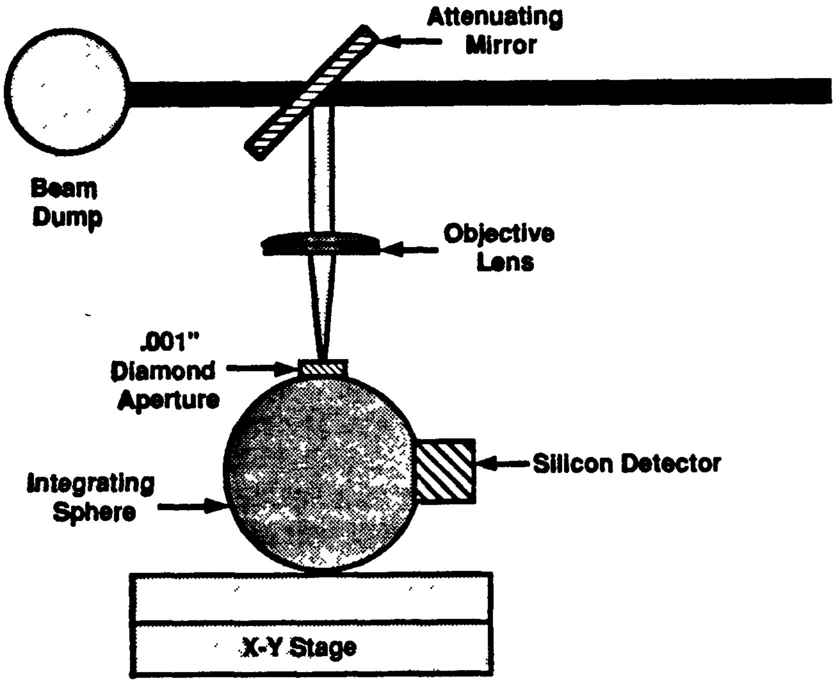

Figure 2.

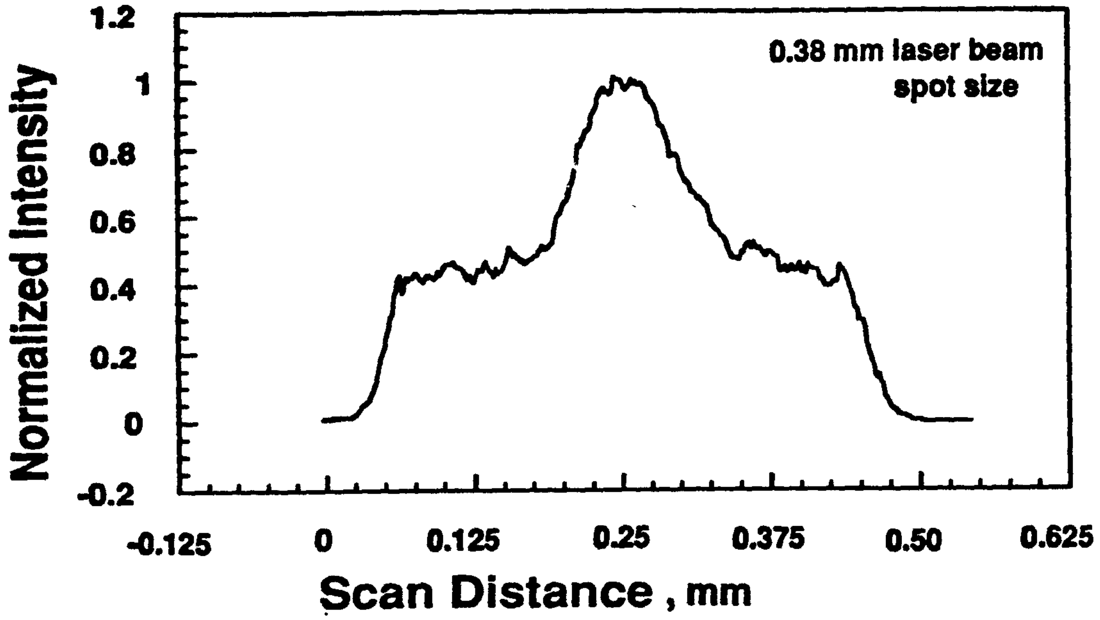

Figure 3.

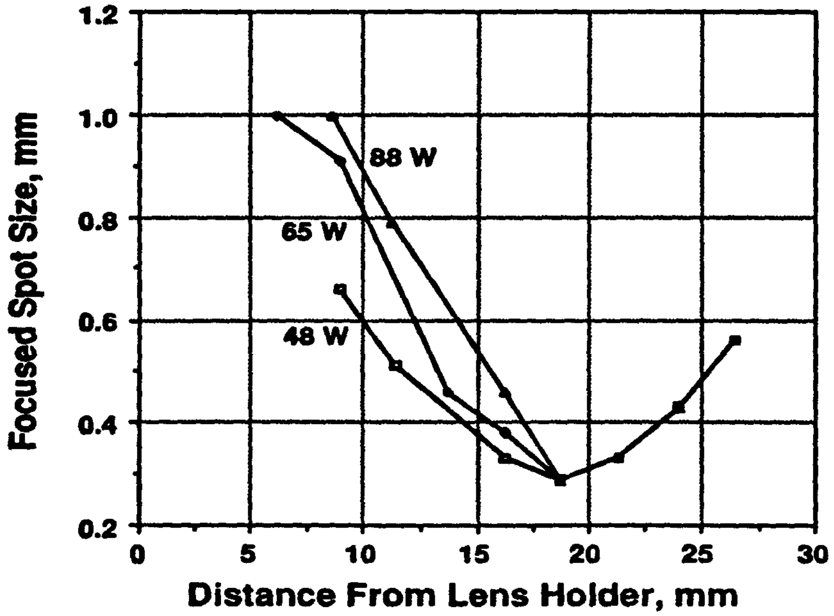

Figure 4.

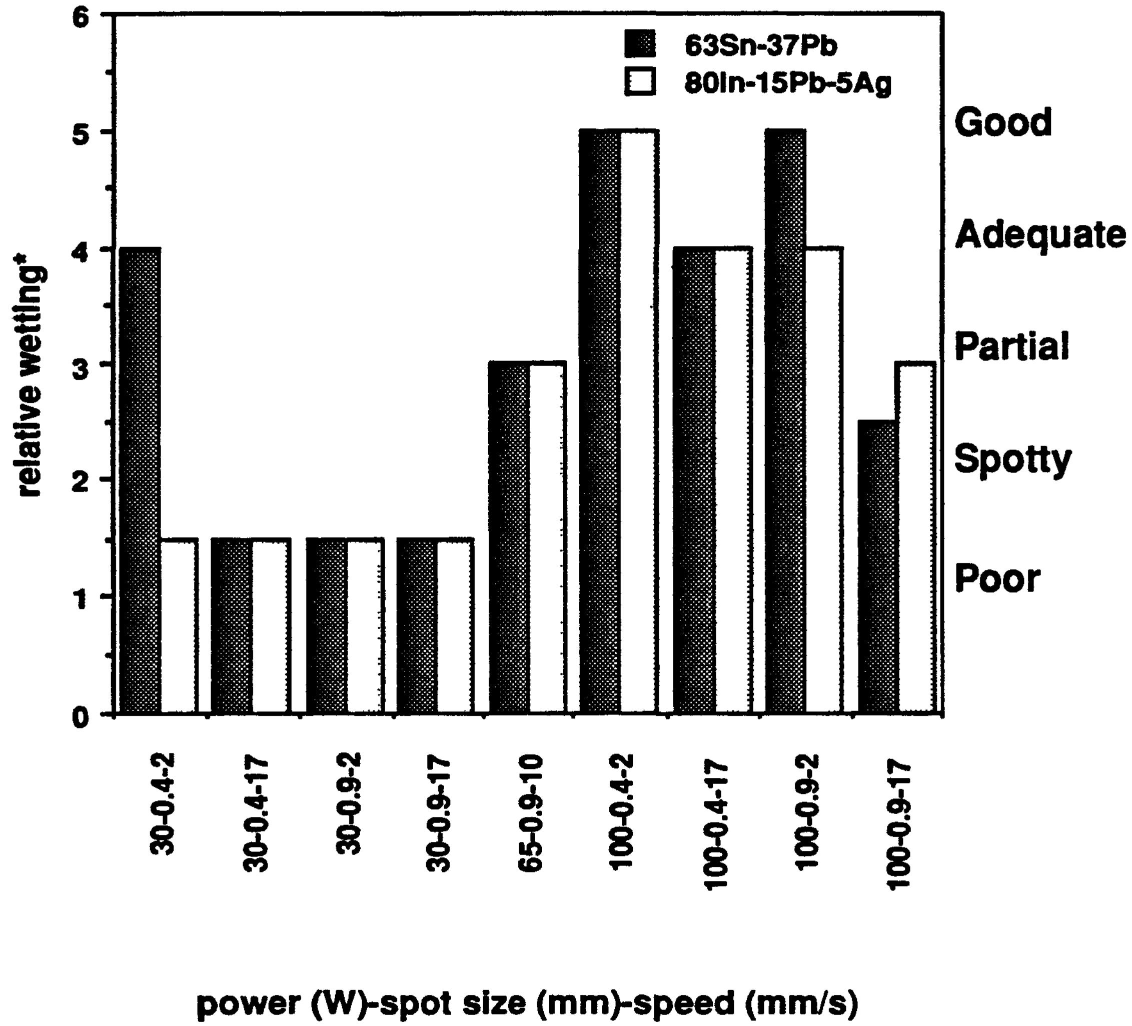

63Sn-37Pb
80In-15Pb-5Ag
relative wetting*
0
1
2
3
4
5
6
Good
Adequate
Partial
Spotty
Poor
30-0.4-2
30-0.4-17
30-0.9-2
30-0.9-17
65-0.9-10
100-0.4-2
100-0.4-17
100-0.9-2
100-0.9-17
power (W)-spot size (mm)-speed (mm/s)

Figure 5.

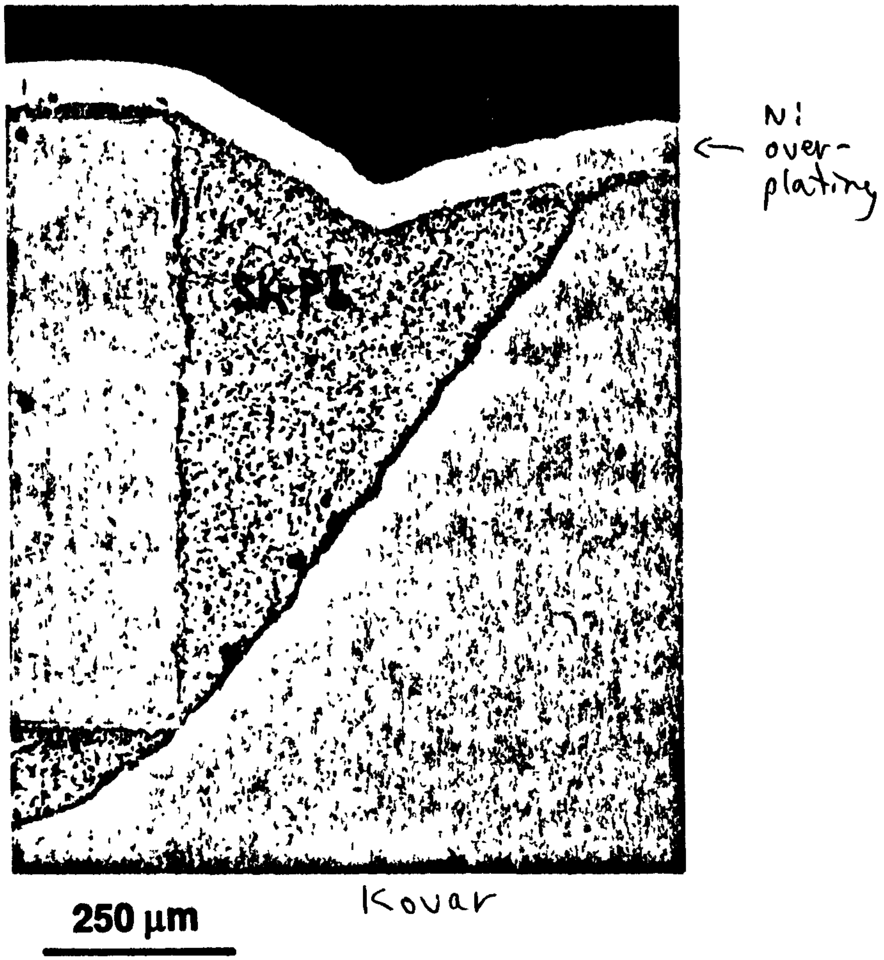

Figure 6a.

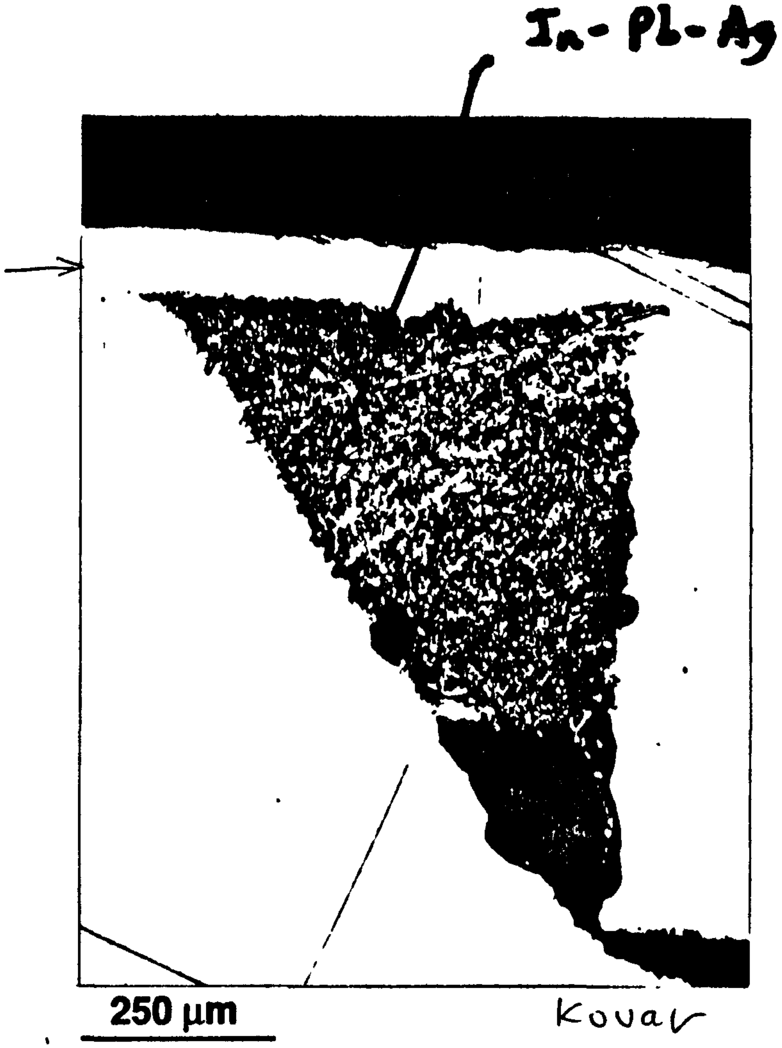

Figure 6b.